

## Determination of the Acidity of MCM-41 with Different Si/Al Ratios by the Temperature Programmed Desorption of Pyridine<sup>†</sup>

Marcelo J.B. Souza<sup>1</sup>, Stevie H. Lima<sup>2</sup>, Antonio S. Araujo<sup>2\*</sup>, Anne M. Garrido Pedrosa<sup>2</sup> and Ana C.S.L.S. Coutinho<sup>2</sup> (1) Department of Chemical Engineering, Federal University of Sergipe, 49100-000, São Cristovão, SE, Brazil. (2) Department of Chemistry, Federal University of Rio Grande do Norte, 59078-970, Natal, RN, Brazil.

**ABSTRACT:** Mesoporous catalysts of MCM-41 type with different Si/Al ratios were synthesized by the hydrothermal method and characterized by X-ray diffraction, nitrogen adsorption and thermogravimetric analysis. Their acidic properties were determined via the temperature programmed desorption of pyridine. Vyazovkin kinetic models were used to correlate the total acidity as a function of the Si/Al ratio with the apparent activation energy for pyridine desorption. The results obtained indicated that the catalysts possessed weak and medium acidic sites. An increase in the Si/Al ratio led to an increase in the activation energy for pyridine desorption.

## INTRODUCTION

MCM-41 is a synthetic molecular sieve whose pore structure consists of hexagonally packed cylinders (Zhao *et al.* 1996; Beck *et al.* 1992). This kind of nano-structured material has been studied quite extensively due its potential applications in catalytic and adsorption processes. Hexagonal mesoporous systems with high surface areas allow the possibility of generating the surface acidity necessary to catalyze the organic reactions employed in the petroleum industry. Studies involving the incorporation of aluminium into the structure of mesoporous materials have also been undertaken (Busio *et al.* 1995; Cesteros and Haller 2001).

Studies of the acidic properties of molecular sieves reported in the literature have employed several techniques such as infrared absorption spectroscopy, temperature programmed desorption and thermogravimetry. Such techniques allow the determination of the density, strength and nature of the acid sites. n-Butylamine has been widely used as a probe molecule in the characterization of the acidic character of the adsorbents and catalysts (Pedrosa *et al.* 2006; Souza *et al.* 2004), its adsorption and subsequent thermodesorption being employed to determine the acid strength and density of several materials. The total acidity of catalysts is an important parameter that assists in the interpretation of their activity and selectivity.

In the present work, a comparative study of the acidic properties of a series of AlMCM-41 materials with different silicon/aluminium ratios is reported. The results obtained were correlated using a model-free (Vyazovkin and Lesnikovic 1988; Vyazovkin and Goryachko 1992) kinetic model in order to evaluate the influence of the silicon/aluminium ratio and the total acidity on the apparent activation energy for pyridine desorption as a function of the degree of desorption.

<sup>†</sup>First presented at the 6th Brazilian Meeting on Adsorption held in Maringá, State of Paraná, Southern Brazil on August 13–16, 2006.

\*Author to whom all correspondence should be addressed. E-mail: asa-ufrn@usa.net.

## EXPERIMENTAL

### Synthesis and characterization procedure

AlMCM-41 materials were synthesized using tetramethylammonium silicate (TMAS, Sigma-Aldrich) as the silicon source, sodium hydroxide (Vetec) as the sodium source, pseudo-bohemite (Vista) as the aluminium source, cetyltrimethylammonium bromide (CTMABr, Vetec) as the template structure and distilled water as the solvent (Araujo *et al.* 2004). For pH adjustment, 30% acetic acid in ethanol solution was employed. The chemicals were mixed in the appropriate proportions necessary to obtain a gel with the molar composition  $4.58\text{SiO}_2 \cdot (0.437 + x)\text{Na}_2\text{O} \cdot 1\text{CTMABr} \cdot x\text{Al}_2\text{O}_3 \cdot 200\text{H}_2\text{O}$ . The quantity  $x$  is the molar composition relative to the aluminium source. The value of  $x$  was varied as 0.114, 0.0570, 0.0380 and 0.0285 in order to obtain materials with silicon/aluminium atomic ratios of 20, 40, 60 and 80, respectively, the corresponding materials being designated as AlMCM-41(20), AlMCM-41(40), AlMCM-41(60) and AlMCM-41(80), respectively. The hydrogels were placed in a 45 mL, Teflon-lined autoclave and heated at 100°C for 3 d. Their pH values were measured each day and adjusted to a value in the range 9–10. On the third day, sodium acetate (Carlo Erba) was added in a 1:3 molar proportion to  $\text{CH}_3\text{COONa}/\text{CTMABr}$  in order to stabilize the silica (Araujo *et al.* 2000). The materials thus obtained were filtered, washed and dried in an oven at 100°C for 2 h. The resulting materials were calcined at 450°C for 1 h in nitrogen and for an additional hour in air at a heating rate of 5°C/min in agreement with the procedure described previously (Souza *et al.* 2004; Araujo *et al.* 2004). The acid forms of the AlMCM-41 materials were obtained by two successive refluxes of ca. 0.5 g of each material with a 0.6 M solution of  $\text{NH}_4\text{Cl}$  for 2 h at 60°C followed by calcination at 450°C in a nitrogen atmosphere for 1 h.

XRD measurements were undertaken on a Shimadzu instrument using Cu K $\alpha$  radiation at a 2 $\theta$  angle in the range of 1–10° employing steps of 0.01°. The surface areas, pore volumes and pore-size distributions of the samples were obtained by BET (Brunauer *et al.* 1938) and BJH (Barrett *et al.* 1951) methods employing nitrogen adsorption isotherms obtained at –196°C (Nova 2000 instrument). TG analysis was undertaken using Mettler equipment (TGA/SDTA851 model) with nitrogen as the gas carrier at a flow rate of 25 mL/min.

### Pyridine adsorption procedure

Pyridine adsorption experiments on the AlMCM-41 samples were performed in a reactor containing ca. 0.1 g of catalyst, which had initially been activated by heating at 400°C under a nitrogen flow of 100 mL/min for 2 h. After such activation, the temperature was reduced to 95°C and the nitrogen flow was diverted to a bubbler flask containing liquid pyridine. The resulting nitrogen stream saturated with pyridine vapour was allowed to flow through the reactor containing the samples for 40 min. After this time, the sample was subjected to a flow of pure nitrogen gas for an additional 40 min to remove the physically adsorbed pyridine. Pyridine desorption was performed by TG analysis, the samples being heated from room temperature up to 900°C at heating rates of 5, 10 and 20°C/min. Vyazovkin kinetic models (Vyazovkin and Lesnikovic 1988; Vyazovkin and Goryachko 1992) were used to evaluate the apparent activation energy as a function of the degree of pyridine desorption.

RESULTS AND DISCUSSION

The adsorption parameters obtained are listed in Table 1. The AlMCM-41 materials showed significant values for the BET surface area ( $S_{\text{BET}}$ ),  $a_0$  (mesopore parameter),  $d_p$  (pore diameter), pore volume ( $V_p$ ) and silica–alumina wall thickness ( $W_t$ ) obtained after the synthesis and treatment processes. These properties all show a dependence on the degree of crystallinity as depicted in Figure 1. The degree of crystallinity also increases with the aluminium content of the sample. Samples with a high degree of crystallinity present the highest degree of hexagonal ordination and consequently high values of the specific surface area, pore diameter and pore volume.

Figure 1 shows the X-ray diffractograms for calcined AlMCM-41 samples with different Si/Al ratios. These show that the intensity of the patterns decreased significantly as the silicon/aluminium ratios of the samples increased, with the exception of the sample with an Si/Al ratio of 40. The variation in the XRD intensities is attributed to the different degrees of crystallinity of the samples (Marler *et al.* 1996). Other workers have shown that the incorporation of aluminium

TABLE 1. Adsorption Parameters of the AlMCM-41 Samples Studied

Sample	BET surface area, $S_{\text{BET}}$ (m <sup>2</sup> /g)	Total pore volume, $V_t$ (cm <sup>3</sup> /g)	Mesopore parameter, $a_0$ (nm) <sup>a</sup>	Pore diameter, $d_p$ (nm)	Wall thickness, $W_t$ (nm) <sup>b</sup>
AlMCM-41(20)	803	0.47	4.18	2.32	1.86
AlMCM-41(40)	894	0.58	4.16	2.59	1.57
AlMCM-41(60)	658	0.38	4.23	2.12	2.11
AlMCM-41(80)	525	0.35	4.39	2.72	1.67

<sup>a</sup> $a_0 = 2d_{(100)}/\sqrt{3}$ ; <sup>b</sup> $W_t = a_0 - d_p$ .

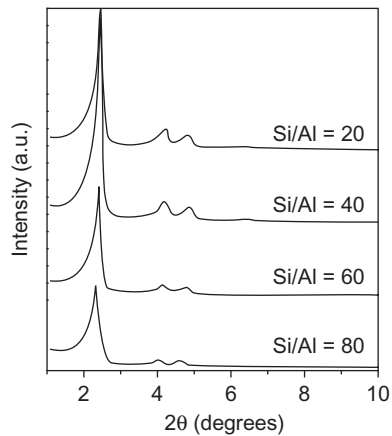


Figure 1. XRD powder patterns of AlMCM-41 with different silicon/aluminium ratios.

into MCM-41 materials leads to higher degrees of crystallinity than occur in pure siliceous MCM-41 due to the formation of materials with a higher structural stability (Shen and Kavi 1999; Araujo and Jaroniec 2000). All the materials showed characteristic peaks in the  $2\theta$  range of  $1\text{--}10^\circ$ , which could be related to the (100), (110) and (210) Miller indices characteristic of AlMCM-41 materials (Zhao *et al.* 1996; Beck *et al.* 1992).

Thermogravimetric analysis of pyridine desorption from HAlMCM-41 materials showed typically two mass losses. The first at  $30\text{--}100^\circ\text{C}$  was attributed to the loss of physisorbed water and pyridine, while the second at  $100\text{--}260^\circ\text{C}$  was attributed to the loss of pyridine chemisorbed onto the acid centres in the HAlMCM-41 structure. Comparison of the temperature range for pyridine desorption with those obtained from experiments performed on zeolites using similar bases (Kofke *et al.* 1989; Silva *et al.* 2004; Araujo and Jaroniec 2000) suggested that the acid centres were of weak to medium strength. The total acidity was measured from the weight loss of chemisorbed pyridine ( $X_{\text{pyr}}$ ) over the temperature range  $100\text{--}260^\circ\text{C}$ , taking consideration of the fact that each pyridine molecule adsorbs at only one acid centre. Table 2 shows the values of the weight loss observed in the TG analysis of the HAlMCM-41 samples with different Si/Al ratios. These experiments were carried out at a heating rate of  $10^\circ\text{C}/\text{min}$ .

TG experiments were also performed at heating rates of 5 and  $20^\circ\text{C}/\text{min}$  in order to evaluate the activation energy for pyridine desorption from the HAlMCM-41 materials. In a typical model-free experiment, the rate of a reaction depends on the degree of conversion ( $\alpha$ ), the temperature ( $T$ ) and the time ( $t$ ) [equation (1)]:

$$\ln\left(\frac{\beta}{t_\alpha^2}\right) = \ln\left[\frac{Rk_0}{E_\alpha g(\alpha)}\right] - \frac{E_\alpha}{R} \frac{1}{T_\alpha} \quad (1)$$

Thus, it is necessary to employ at least three different heating rates ( $\beta$ ), with the respective conversion curves being evaluated from the measured TG curves. Thus, for each degree of conversion ( $\alpha$ ), the quantity  $\ln(\beta/t_\alpha^2)$  is plotted against  $1/T_\alpha$  to provide a straight line with the slope  $-E_0/R$  (Figure 2). This allows the activation energy to be obtained as a function of the degree of conversion (Figure 3).

As can be observed from the data listed in Table 2, increasing the Si/Al ratio led to a decrease in the total acidity with values of 1.2, 0.93, 0.82 and 0.43 mmol/g being obtained for Si/Al ratios of 20, 40, 60 and 80, respectively. The very small superficial acidity of ca. 0.11 mmol/g exhibited by the parent MCM-41 material is probably due to structural defects and non-condensed surface silanol groups. Analysis by the model-free kinetic approach showed that, as the Si/Al ratio of the

**TABLE 2.** Total Acidity, Weight Loss (%) and Respective Temperatures Ranges for Pyridine Desorption from HAlMCM-41 Materials with Different Si/Al Ratios

Sample	Temperature range ( $^\circ\text{C}$ )			Total acidity (mmol pyridine/g)
	30–100	100–260	30–260	
HAlMCM-41(20)	3.63	1.20	4.83	1.20
HAlMCM-41(40)	3.48	0.93	4.41	0.93
HAlMCM-41(60)	3.43	0.82	4.25	0.82
HAlMCM-41(80)	5.09	0.43	5.52	0.43
SiMCM-41	2.12	0.11	2.23	0.11

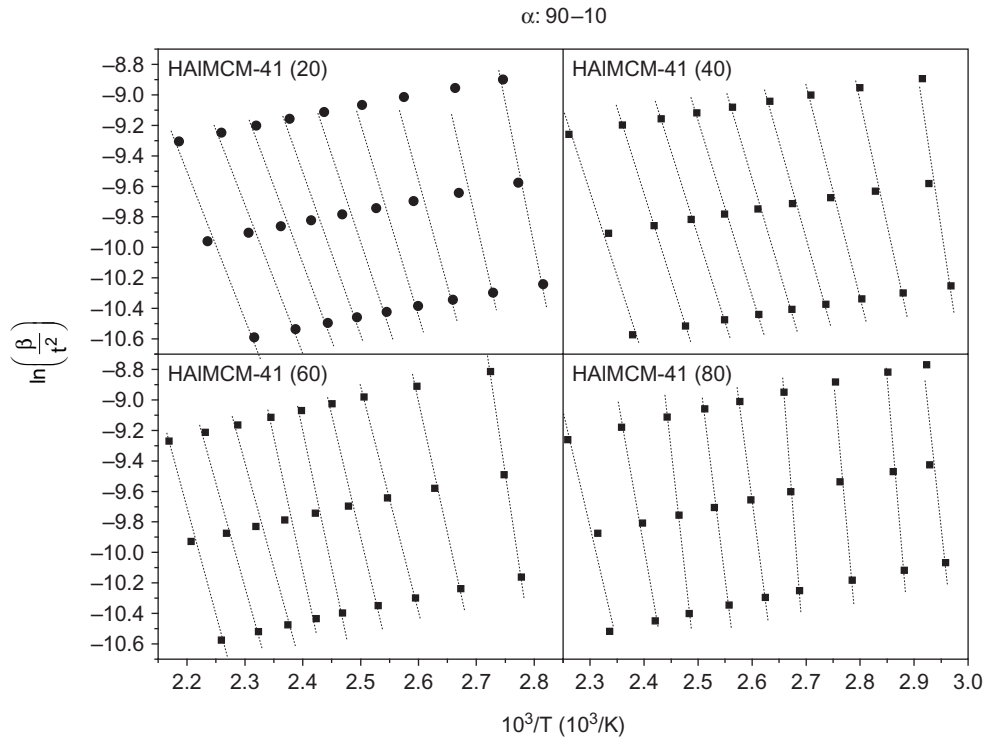


**Figure 2.** Kinetic curves for pyridine desorption from HAlMCM-41 samples with Si/Al ratios of 20, 40, 60 and 80 as obtained employing the model-free kinetic approach.

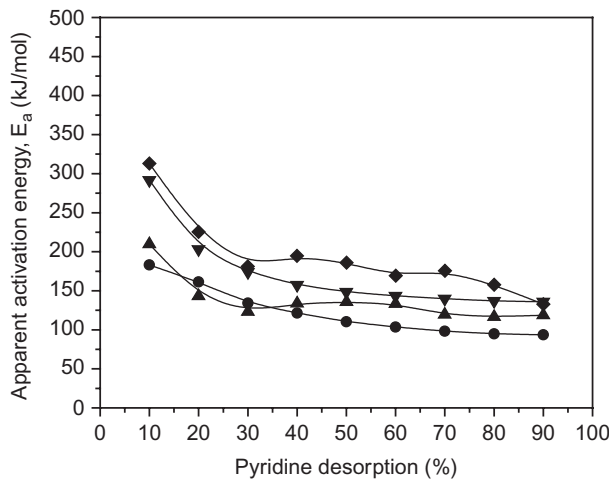


**Figure 3.** Apparent activation energy curves as a function of pyridine desorption obtained using the model-free kinetic approach. Data points relate to the following samples: ●, HAlMCM-41 (20); ▲, HAlMCM-41 (40); ▼, HAlMCM-41 (60); ◆, HAlMCM-41 (80).

samples increased, an increase also occurred in the apparent activation energy necessary to desorb the pyridine from the acid sites (Figure 3). These results suggest that high aluminium concentrations increase the total acidity, but that the acid strength of the individual sites diminishes under these circumstances. The change in the apparent activation energy during the desorption of 5–30% pyridine probably arose from applying the model to measurements which were outside its limits of applicability.

## CONCLUSIONS

AlMCM-41 nanoporous materials with different Si/Al ratios were successfully synthesized using the hydrothermal method. The use of pyridine as a probe molecule to evaluate the total acidity proved satisfactory. The materials studied exhibited adsorption sites with typically weak to medium acid strengths with values of 1.2, 0.93, 0.82 and 0.43 mmol/g total acidity at Si/Al ratios of 20, 40, 60 and 80, respectively. The model-free kinetic approach was applied to determine the apparent activation energy for pyridine desorption. This showed that an increase in the apparent activation occurred as the Si/Al ratio of the sample increased. These results suggest that high aluminium concentrations increase the total acidity but decrease the relative acid strengths of the acid sites.

## ACKNOWLEDGEMENTS

The authors thank Conselho Nacional de Desenvolvimento Científico e Tecnológico (Edital Universal, Proc. 472111/2006-0/MCT/CNPq) for support.

## REFERENCES

- Araujo, A.S. and Jaroniec, M. (2000) *Thermochim. Acta* **345**, 173.
- Araujo, A.S., Fernandes, Jr., V.J., Souza, M.J.B., Silva, A.O.S. and Aquino, J.M.F.B. (2004) *Thermochim. Acta* **413**, 235.
- Barrett, E.P., Joyner, L.J. and Halenda, P. (1951) *J. Am. Chem. Soc.* **73**, 373.
- Beck, J.S., Vartuli, J.C., Roth, W.J., Leonowicz, M.E., Kresge, C.T., Schmitt, K.D., Chu, C.T.W., Olson, D.H., Sheppard, E.W., McCullen, S.B., Higgins, Y.B. and Schlenker, I. L. (1992) *J. Am. Chem. Soc.* **114**, 10 834.
- Brunauer, S., Emmett, P.H. and Teller, E. (1938) *J. Am. Chem. Soc.* **60**, 309.
- Busio, M., Jänchen, J., and Van Hooff, J.H.C. (1995) *Microporous Mesoporous Mater.* **5**, 211.
- Cesteros, Y. and Haller, G.L. (2001) *Microporous Mesoporous Mater.* **43**, 171.
- Marler, B., Oberhagemann, U., Vortmann, S. and Gies, H. (1996) *Microporous Mesoporous Mater.* **6**, 375.
- Kofke, T.J.G., Gorte, R.J., Kokotailo, G.T. and Farneth, W.E. (1989) *J. Catal.* **115**, 265.
- Pedrosa, A.M.G., Souza, M.J.B., Melo, D.M.A. and Araujo, A.S. (2006) *Mater. Res. Bull.* **41**, 1105.
- Shen, S.C. and Kavi, S. (1999) *J. Phys. Chem. B* **103**, 8870.
- Silva, A.O.S., Souza, M.J.B., Aquino, J.M.F.B., Fernandes, Jr., V.J. and Araujo, A.S. (2004) *J. Therm. Anal. Calorim.* **75**, 699.
- Souza, M.J.B., Silva, A.O.S., Aquino, J.M.F.B., Fernandes, Jr., V.J. and Araujo, A.S. (2004) *J. Therm. Anal. Calorim.* **75**, 693.
- Vyazovkin, S. and Lesnikovich, A.I. (1988) *Russ. J. Phys. Chem.* **62**, 2949.
- Vyazovkin, S. and Goryachko, V. (1992) *Thermochim. Acta* **194**, 221.
- Zhao, X.S., Lu, G.Q. and Millar, G.J. (1996) *Ind. Eng. Chem., Res.* **35**, 2075.